Contribution from the Departments of Chemistry, University of Minnesota, Minneapolis, Minnesota 55455, and St. Olaf College, Northfield, Minnesota 55057

Di- and Trithiocarbamato Complexes of Osmium(III) and the Crystal and Molecular Structure of $[Os_2(SeS_2CNMe_2)_2(S_2CNMe_2)_3]PF_6$

L. J. MAHEU, G. L. MIESSLER, J. BERRY, M. BUROW, and L. H. PIGNOLET*

Received April 26, 1982

Di- and trithiocarbamate complexes of osmium have been studied. A novel (selenodithiocarbamato)diosmium complex has also been synthesized, $[Os_2(\mu\text{-}SeS_2CNMe_2)_2(S_2CNMe_2)_3]PF_6$, and characterized by single-crystal X-ray diffraction: space group $P\bar{1}$; unit cell dimensions a = 6.381 (2) Å, b = 15.590 (3) Å, c = 21.115 (6) Å, α = 96.87 (2)°, β = 93.10 (3)°, γ = 91.43 (2)°; R = 8.3%. The selenium atoms occupy the bridging positions, but otherwise, this complex is very similar to its trithiocarbamate analogue $[Os_2(\mu\text{-}S_3CNMe_2)_2(S_2CNMe_2)_3]PF_6$. The mechanism of sulfur and selenium incorporation into $Os(S_2CNR_2)_3$ probably involves initial bonding and activation of S_8 or Se_8 by osmium. The bimetallic complex $[Os_2(S_2CNMe_2)_5]Cl$ has been shown to have two isomeric structures, which thermally interconvert in a manner that is similar to that of the ruthenium analogues. Also, $Os(S_2CNR_2)_3$ complexes are stereochemically nonrigid, and the trigonal twist mechanism has been shown to be operative by proton NMR spectroscopy. Activation parameters have been determined for this rearrangement in $Os[S_2CN(benzyl)_2]_3$ and are very similar to those of the ruthenium analogue.

Introduction

Recent results from our laboratory have demonstrated the existence of trithiocarbamato complexes of osmium(III).[1,2] Complexes **1** and **2** were synthesized by reaction of elemental

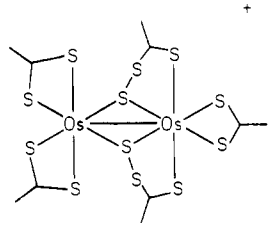

1, $[Os_2(S_3CNMe_2)_2(S_2CNMe_2)_3]^+$

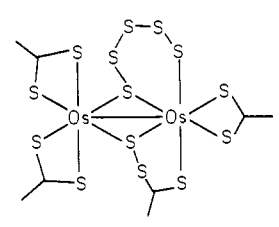

2, $[Os_2(S_5)(S_3CNEt_2)(S_2CNEt_2)_3]$

sulfur with $Os(S_2CNR_2)_3$, R = Me and Et, and have been characterized by single-crystal X-ray diffraction.[2] These complexes are important since they represent the only known examples of the trithiocarbamate ligand,[3] and this ligand has been proposed to be a key intermediate in the dithiocarbamate acceleration of rubber vulcanization.[4,5] Because of the potential importance of these compounds in sulfur transport,[6] experiments have been carried out with elemental selenium in place of elemental sulfur in order to determine the site or sites of selenium addition. The results of this experiment are reported here and discussed in terms of the mechanism of sulfur incorporation.

Complexes such as **1** but without the two extra sulfur atoms are also known but have never been structurally characterized.[7] The complex $[Os_2(S_2CNMe_2)_5]^+$ has been found to undergo an isomerization reaction at 78 °C in CD_3CN solution. The rate of this reaction has been measured by ^1H NMR techniques. From comparison with the analogous ruthenium complexes,[8] it is suggested that $[Os_2(S_2CNMe_2)_5]^+$ exists in the α, **3**, and β, **4**, forms with the β form being the more stable. These results are presented here.

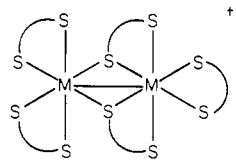

3, α-$[M_2(S_2CNMe_2)_5]^+$

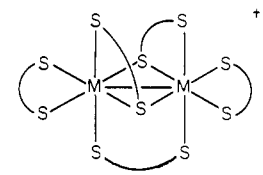

4, β-$[M_2(S_2CNMe_2)_5]^+$

The stereochemical nonrigidity of tris chelate metal complexes has received considerable attention over the past several years.[9-11] Mechanistic and kinetic information on the modes of rearrangement for various octahedral tris chelate complexes has been obtained through the use of dynamic nuclear magnetic resonance (DNMR).[9-11] One class of compounds that has been extensively studied is the tris(diorganodithiocarbamate) complexes, $M(S_2CNR_2)_3$.[12-17] We have been particularly interested in the metal-centered rearrangements of iron and ruthenium tris(diorganodithiocarbamato) complexes.[12-15,17] These complexes were shown to rearrange exclusively by the trigonal twist mechanism.[12-15,17,18] This mechanism leads only to enantiomerization, and kinetic parameters for this process have been obtained for the iron and ruthenium tris chelates by comparison of computer-simulated spectra to the actual spectra.[15,17,18] At higher temperatures geometrical isomerization of the unsymmetrically substituted tris chelates of iron and ruthenium results from rapid S_2C–N bond rotation.[12-15,17,18]

As an extension of our previous work in this area, a study of the DNMR properties of $Os(S_2CNBz_2)_3$, Bz = benzyl, and

* To whom correspondence should be addressed at the University of Minnesota.

(1) Maheu, L. J.; Pignolet, L. H. *Inorg. Chem.* **1979**, *18*, 3626.
(2) Maheu, L. J.; Pignolet, L. H. *J. Am. Chem. Soc.* **1980**, *102*, 6346.
(3) A trithiocarbamate complex of ruthenium(III), $Ru(S_3CNMe_2)(S_2CNMe_2)_2$, has recently been prepared in our laboratory. See: Maheu, L. J. Ph.D. Thesis, University of Minnesota, Minneapolis, MN, 1981.
(4) Coleman, M. M.; Shelton, J. R.; Koenig, J. L. *Ind. Eng. Chem. Prod. Res. Dev.* **1974**, *13*, 154.
(5) Allen, P. W.; Barnard, D.; Saville, B. *Chem. Br.* **1970**, *6*, 382.
(6) Fackler, J. P., Jr.; Fetchin, J. A.; Fries, D. C. *J. Am. Chem. Soc.* **1972**, *94*, 7323 and references cited therein.
(7) Given, K. W.; Wheeler, S. H.; Jick, B. S.; Maheu, L. J.; Pignolet, L. H. *Inorg. Chem.* **1979**, *18*, 1261.
(8) Wheeler, S. H.; Mattson, B. M.; Miessler, G. L.; Pignolet, L. H. *Inorg. Chem.* **1978**, *17*, 340.
(9) Fortman, J. J.; Sievers, R. E. *Coord. Chem. Rev.* **1971**, *6*, 331.
(10) Pignolet, L. H.; Lewis, R. A.; Holm, R. H. *Inorg. Chem.* **1972**, *11*, 99.
(11) Pignolet, L. H.; LaMar, G. H. In "Chemical Applications of NMR in Paramagnetic Molecules"; LaMar, G. N., Horrocks, W. D., Jr., Holm, R. H., Eds.; Academic Press: New York, 1973; Chapter 8.
(12) Palazzotto, M. C.; Pignolet, L. H. *J. Chem. Soc., Chem. Commun.* **1972**, 6.
(13) Duffy, D. J.; Pignolet, L. H. *Inorg. Chem.* **1972**, *11*, 2843.
(14) Pignolet, L. H.; Duffy, D. J.; Que, L., Jr. *J. Am. Chem. Soc.* **1973**, *95*, 295.
(15) Palazzotto, M. C.; Duffy, D. J.; Edgar, B. L.; Que, L., Jr.; Pignolet, L. H. *J. Am. Chem. Soc.* **1973**, *95*, 4537.
(16) Que, L., Jr.; Pignolet, L. H. *Inorg. Chem.* **1974**, *13*, 351.
(17) Duffy, D. J.; Pignolet, L. H. *Inorg. Chem.* **1974**, *13*, 2045 and references cited therein.
(18) Pignolet, L. H. *Top. Curr. Chem.* **1975**, *56*, 91.

0020-1669/83/1322-0405$01.50/0

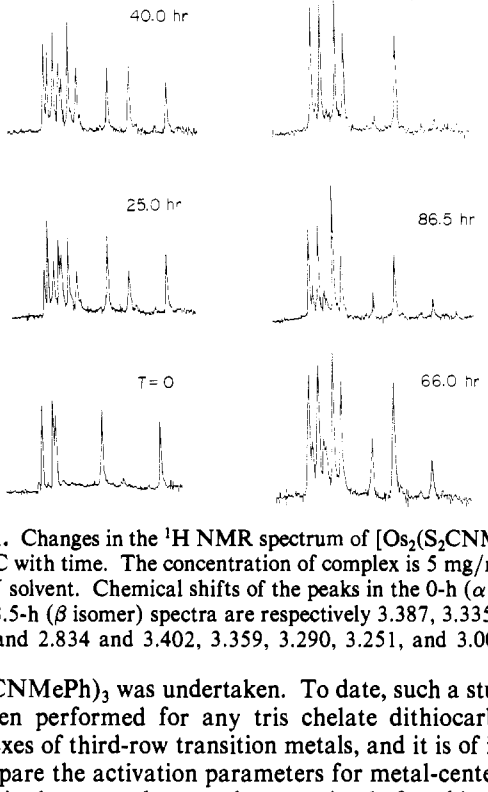

Figure 1. Changes in the ^{1}H NMR spectrum of $[Os_2(S_2CNMe_2)_5]Cl$ at 78 °C with time. The concentration of complex is 5 mg/mL with CD_3CN solvent. Chemical shifts of the peaks in the 0-h (α isomer) and 118.5-h (β isomer) spectra are respectively 3.387, 3.335, 3.323, 3.108, and 2.834 and 3.402, 3.359, 3.290, 3.251, and 3.007 ppm.

$Os(S_2CNMePh)_3$ was undertaken. To date, such a study has not been performed for any tris chelate dithiocarbamate complexes of third-row transition metals, and it is of interest to compare the activation parameters for metal-centered inversion in these complexes to those previously found in the iron and ruthenium systems.

Experimental Section

Preparation of Compounds. **$Os(S_2CNMe_2)_3$** and **$Os(S_2CNEt_2)_3$** were prepared by literature methods.[7] **$Os(S_2CNBz_2)_3$** was prepared according to the literature preparation of $Os(S_2CNEt_2)_3$,[7] reacting $(NH_4)_2OsCl_6$ with an eightfold molar excess of NaS_2CNBz_2 in a 1:1 H_2O–CH_3OH solution under a N_2 atmosphere. The crude reaction product was purified by chromatography on alumina (Alcoa F-20), eluting the deep red-orange band with CH_2Cl_2. The $Os(S_2CNBz_2)_3$ was obtained as dark red crystals by recrystallization from a CH_2Cl_2–heptane solution in the dark;[19] mp 206 °C (uncor). Electronic absorption spectrum (CH_2Cl_2, 25 °C): λ_{max} 243 nm (log ϵ 4.70), 320 sh (3.75), 350 sh (3.93), 385 (4.11), 490 sh (3.47). ^{1}H NMR (25 °C, acetone-d_6 solution): δ(N-CH_2) 16.82, 13.68. Anal. Calcd for $C_{45}H_{42}N_3S_6Os$: C, 53.67; H, 4.17; N, 4.17. Found: C, 53.87; H, 4.34; N, 4.13.

$Os(S_2CNMePh)_3$ was also prepared according to the literature method for $Os(S_2CNEt_2)_3$, using $NaS_2CNMePh$ instead of NaS_2CNEt_2. The crude reaction product was chromatographed on silica gel with 9:1 (v/v) Et_2O–CH_2Cl_2 as eluent. Heptane was added to the collected eluate, and a crystalline, dark red product was obtained by slow evaporation of the solvent;[20] mp 239 °C (uncor). Electronic absorption spectrum (CH_2Cl_2, 25 °C): λ_{max} 250 nm (log ϵ 4.62), 277 sh (4.57), 350 sh (3.96), 385 (3.97), 493 sh (3.34). Anal. Calcd for $C_{24}H_{24}N_3S_6Os$: C, 39.11; H, 3.28; N, 5.70. Found: C, 38.93; H, 3.17; N, 5.55.

α-$[Os_2(S_2CNMe_2)_5]Cl$ was prepared by the literature method for $[Os_2(S_2CNMe_2)_5]Cl$.[7] The characterization data for this compound are presented in ref 7. Its ^{1}H NMR spectrum and that of the β isomer are presented in Figure 1. See Results and Discussion for details of the α to β isomerization.

$[Os_2(\mu\text{-}SeS_2CNMe_2)_2(S_2CNMe_2)_3]PF_6$ was prepared in ca. 10% yield by a method similar to that described for $[Os_2(\mu\text{-}S_3CNMe_2)_2(S_2CNMe_2)_3]PF_6$,[2] except that red selenium (Se_8) was used in place of elemental sulfur. ^{1}H NMR (CD_3CN, ambient): δ 3.633, 3.406, 3.278, 3.252, 3.001. All peaks are singlets of equivalent area. IR: $\nu(S_2CN)$ = 1530 cm^{-1}. Electronic absorption spectrum (CH_3CN, 25 °C): λ_{max} 255 nm (log ϵ 4.62), 365 sh (3.93), 550 (3.01), 928 br (2.15).

Table I. Summary of Crystal Data and Intensity Collection

compd	$[Os_2(SeS_2CNMe_2)_2(S_2CNMe_2)_3]PF_6$
formula	$Os_2C_{15}H_{30}N_5S_{10}Se_2PF_6$
fw	1284.37
a, Å	6.381 (2)
b, Å	15.590 (3)
c, Å	21.115 (6)
α, deg	96.87 (2)
β, deg	93.10 (3)
γ, deg	91.43 (2)
V, Å^3	2081
Z	2
d(calcd), g/cm^3	2.048
space group	$P\bar{1}$
cryst dimens, mm	0.05 × 0.15 × 0.35
temp, °C	23
radiation	Mo Kα (0.710 69 Å) from monochromator
linear abs coeff, cm^{-1}	83.4
max, min transmission factors	0.99, 0.57
2θ limits, deg	0–48
unique data collected (hemisphere)	6438 ($+h,\pm k,\pm l$)
final no. of variables	270
unique data used	3323, $F_o^2 \geq 2.5\sigma(F_o^2)$
R^a	0.083
$R_w{}^a$	0.090
GOF	2.12

^{a} The function minimized was $\Sigma w(|F_o| - |F_c|)^2$, where $w = 1/\sigma^2(F_o)$. The unweighted and weighted residuals are defined as $R = (\Sigma||F_o| - |F_c||)/\Sigma|F_o|$ and $R_w = [(\Sigma w(|F_o| - |F_c|)^2/(\Sigma w|F_o|)^2]^{1/2}$. The GOF is $[\Sigma w(|F_o| - |F_c|)^2/(NO - NV)]^{1/2}$, where NO and NV are the number of observations and variables, respectively.

^{1}H NMR Measurements. All spectra were recorded on a Varian HFT 80 instrument equipped with a variable-temperature probe and deuterium lock. Temperatures were measured by a thermocouple mounted in an NMR tube and are accurate to ±1 °C. Samples of $Os(S_2CNBz_2)_3$ and $Os(S_2CNMePh)_3$ were purified by chromatography (vide supra) immediately before use. Samples ca. 0.1 M in complex were prepared in acetone-d_6 or CD_2Cl_2 and sealed in NMR tubes under a N_2 atmosphere. Chemical shifts are reported in ppm relative to Me_4Si (δ 0.0) with positive shifts downfield.

Kinetic Analysis. A total line-shape analysis, TLSA, was performed for $Os(S_2CNBz_2)_3$. This complex possesses diastereotopic N-CH_2 protons that give two separate resonances in the limit of slow optical inversion (vide infra). Spin–spin coupling is not observed due to the paramagnetic broadening. Coalescence of these two resonances results from metal-centered inversion. A simple two-site exchange was used, and exchange-broadened line shapes were calculated by using the rigorous Gutowsky–Holm equation.[21] Best computer fits were visually selected; these are included as supplementary material. Line widths at half-height, $H_{1/2}$, and chemical shift separations, $\Delta\nu$, were determined in the coalescence region by linear extrapolation from slow-exchange values of the plots of ln $H_{1/2}$ vs. $1/T$ and $\Delta\nu$ vs. $1/T$. This procedure has previously been applied for paramagnetic complexes.[11,17] These plots are included as supplementary material. The rate constant for optical inversion, k (s^{-1}), is defined as τ^{-1}, where τ is the preexchange lifetime of a proton in either environment (τ used here equals 2τ in the Gutowsky–Holm equation).[21] Activation parameters, $\Delta H^\ddagger$ and $\Delta S^\ddagger$, were determined by a least-squares fit to a ln (k/T) vs. $1/T$ plot included as supplementary material. The usual assumption of unity for the transmission coefficient in the Eyring equation was made. Errors were estimated from error limits in k and T. Values of $\Delta G^\ddagger$ in the region of coalescence have comparatively small errors and are therefore the best to use for comparative purposes. $\Delta G^\ddagger$ for $Os(S_2CNBz_2)_3$ was calculated at 46.2 °C from the relation $k = (k_BT/h)\exp(-\Delta G^\ddagger/RT)$.

Structure Determination. Crystals of $[Os_2(\mu\text{-}SeS_2CNMe_2)_2(S_3CNMe_2)_3]PF_6$ were obtained by slow evaporation of a CH_3CN–

(19) Given, K. W. Ph.D. Thesis, University of Minnesota, Minneapolis, MN, 1978; *Diss. Abstr. Int. B* **1979**, *39*, 4380.
(20) Maheu, L. J. Ph.D. Thesis, University of Minnesota, Minneapolis, MN, 1981.
(21) Gutowsky, H. S.; Holm, C. H. *J. Chem. Phys.* **1956**, *25*, 1288.

Table II. Positional and Thermal Parameters and Their Estimated Standard Deviations

atom	x	y	z	B,[a] Å²	atom	x	y	z	B,[a] Å²
Os1	0.4567 (2)	0.14848 (9)	0.32378 (6)	2.146	N12	0.292 (4)	−0.162 (2)	0.218 (1)	3.6 (6)
Os2	0.3097 (2)	0.13565 (9)	0.19373 (6)	2.183	N34	0.425 (5)	0.434 (2)	0.233 (2)	5.4 (8)
Se1	0.6382 (6)	0.0909 (3)	0.2341 (2)	3.818	N56	0.648 (5)	0.366 (2)	0.462 (2)	5.2 (8)
Se2	0.1291 (5)	0.1941 (2)	0.2834 (2)	3.392	N78	0.576 (4)	−0.066 (2)	0.425 (1)	3.1 (5)
S1	0.612 (1)	−0.0546 (6)	0.2184 (5)	3.602	N91	0.081 (4)	0.117 (2)	0.004 (1)	3.8 (6)
S2	0.157 (1)	−0.0044 (5)	0.1956 (4)	2.256	C12	0.350 (5)	−0.077 (2)	0.216 (1)	2.4 (6)
S3	0.138 (1)	0.3383 (6)	0.2758 (5)	3.562	C12A	0.430 (8)	−0.223 (3)	0.232 (3)	6.9 (12)
S4	0.461 (1)	0.2731 (6)	0.1827 (4)	2.863	C12B	0.063 (7)	−0.191 (3)	0.209 (2)	5.9 (11)
S5	0.382 (1)	0.2289 (6)	0.4246 (4)	3.265	C34	0.351 (6)	0.346 (3)	0.232 (2)	4.4 (8)
S6	0.659 (1)	0.2815 (6)	0.3375 (4)	2.924	C34A	0.351 (7)	0.507 (3)	0.282 (2)	5.6 (10)
S7	0.719 (1)	0.0818 (6)	0.3885 (4)	3.319	C34B	0.622 (7)	0.447 (3)	0.196 (2)	5.6 (10)
S8	0.305 (1)	0.0168 (5)	0.3539 (3)	2.744	C56	0.573 (5)	0.301 (2)	0.408 (2)	3.0 (7)
S9	0.397 (1)	0.0887 (7)	0.0842 (4)	3.765	C56A	0.570 (7)	0.381 (3)	0.521 (2)	5.9 (10)
S10	0.014 (1)	0.1645 (6)	0.1228 (4)	2.875	C56B	0.836 (7)	0.421 (3)	0.442 (2)	6.1 (11)
P	−0.103 (2)	0.6665 (8)	0.3499 (6)	5.081	C78	0.539 (5)	−0.000 (2)	0.392 (2)	3.1 (7)
F1	0.128 (4)	0.676 (2)	0.340 (2)	9.244	C78A	0.791 (6)	−0.078 (3)	0.453 (2)	4.9 (9)
F2	−0.343 (5)	0.665 (3)	0.360 (1)	10.749	C78B	0.425 (6)	−0.137 (2)	0.425 (2)	3.7 (7)
F3	−0.132 (6)	0.759 (2)	0.342 (2)	9.794	C91	0.152 (7)	0.123 (3)	0.056 (2)	6.4 (11)
F4	−0.071 (7)	0.572 (2)	0.357 (2)	12.131	C91A	0.215 (6)	0.078 (3)	−0.051 (2)	4.7 (9)
F5	−0.069 (5)	0.684 (2)	0.421 (1)	9.273	C91B	−0.135 (7)	0.137 (3)	−0.023 (2)	5.4 (10)
F6	−0.148 (6)	0.651 (2)	0.273 (1)	10.549					

[a] Anisotropic thermal parameters are included as supplementary material.

toluene solution. A small rectangular needle was selected and used for data collection. Relevant crystallographic data are given in Table I. The cell constants were determined by least-squares refinement of the angular settings of 25 Mo Kα (λ = 0.71069 Å) reflections in the 22–30° 2θ range centered on a CAD 4 diffractometer using the Enraf-Nonius automatic peak-searching and centering program.[22] The space group $P\bar{1}$ was used and led to successful solution and refinement. Data collection was carried out on the CAD 4 diffractomer using graphite-monochromatized Mo Kα radiation and employing a variable-rate ω–2θ scan technique. No decrease in the intensities of periodically remeasured reflections was noted. The data were corrected for Lorentz, polarization, background, and absorption (empirical method) effects. Conventional heavy-atom techniques were used to solve the structure, and refinement was carried out with the Os, Se, S, P, and F atoms thermally anisotropic and the remaining non-hydrogen atoms isotropic by full-matrix least-squares methods.[23] In the final difference Fourier map, the highest peak was 1.7 e Å^{-3} and was located ca. 1 Å from Os2. No chemically significant features were noted in this map.

The assignment of the Se atoms to the bridging positions is based on an examination of the values of the thermal parameters, a refinement of the multiplicities of the Se and S atoms, and an examination of the bond distances (vide infra). The thermal parameters

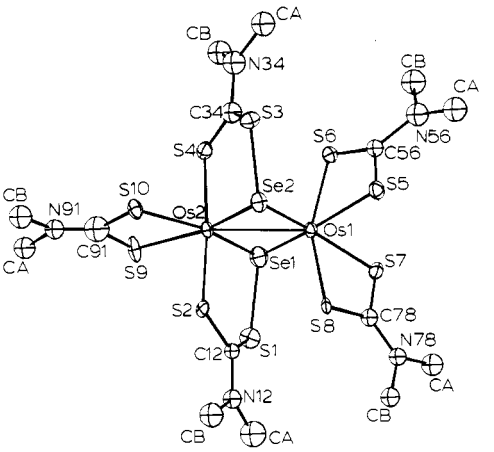

Figure 2. ORTEP drawing of the cation $[Os_2(SeS_2CNMe_2)_2(S_2CNMe_2)_3]^+$. The thermal ellipsoids are drawn with 30% probability boundaries.

for the Se atoms are reasonable with full occupancy assumed for selenium in the bridging positions (see Table II). Refinement calling these atoms sulfur converged to give large negative thermal parameters for the bridge positions (isotropic equivalent B of −4.0 and −3.9 Å² compared with an average value of 3.5 Å² for the ten nonbridging sulfur atoms). When the thermal parameters and multiplicities for the two selenium and ten sulfur atoms were simultaneously refined, the following values were obtained [atom, multiplicity (isotropic equivalent B, Å²)]: Se1, 0.85 (5), 2.8; Se2, 0.91 (5), 3.0; S1, 0.96 (5), 3.4; S2, 1.00 (2), 2.7; S3, 1.10 (5), 4.1; S4, 0.85 (5), 2.1; average for remaining six S atoms, 0.98 (5), 3.0. These values suggest that the bridge positions are at least 90% Se. Some sulfur (<10%) could be incorporated into these positions, but there is no sign of disorder and the S occupancy factors are not unusually high. The final refinement was carried out with all occupancy factors fixed at unity.

The quality of the structure determination is not high (R = 0.083) due to very poor crystal quality. However, extreme difficulty was experienced in obtaining better quality crystals, and the location of the selenium atoms was unambiguously determined. Since this was the primary goal of the structure determination, a decision was made to accept the structure in its present form. Attempts were made to improve the model by refinement with all non-hydrogen atoms anisotropic but, due to the limited data set, failed to significantly improve R and were therefore abandoned. Some disorder in the PF_6 anion was also noted, but a better model was not apparent.

The final atomic coordinates with their estimated standard deviations and the final thermal parameters are given in Table II and as

(22) All calculations were carried out on a PDP 11/34 computer using the Enraf-Nonius SDP programs. This crystallographic computing package is described by: Frenz, B. A. In "Computing in Crystallography"; Schenk, H., Olthof-Hazekamp, R., van Koningsveld, H., Bassi, G. C., Eds.; Delft University Press: Delft, Holland, 1978; pp 64–71.

(23) The intensity data were processed as described in: "CAD4 and SDP User's Manual"; Enraf-Nonius: Delft, Holland, 1978. The net intensity I is given as

$$I = \frac{K}{\mathrm{NPI}}(C - 2B)$$

where K = 20.1166 times the attenuator factor, NPI = ratio of fastest possible scan rate to scan rate for the measurement, C = total count, and B = total background count. The standard deviation in the net intensity is given by

$$\sigma^2(I) = \left(\frac{K}{\mathrm{NPI}}\right)^2[C + 4B + (pI)^2]$$

where p equals 0.05 and is a factor used to downweight intense reflections. The observed structure factor amplitude F_o is given by

$$F_o = (I/Lp)^{1/2}$$

where Lp = Lorentz and polarization factors. The $\sigma(I)$'s were converted to the estimated errors in the relative structure factors $\sigma(F_o)$ by

$$\sigma(F_o) = \tfrac{1}{2}[\sigma(I)/I]F_o$$

Table III. Near-IR Spectral Data for $[M_2(S_2CNMe_2)_5]X$ Complexes

complex	λ_{max}, nm	log ϵ
α-$[Os_2(S_2CNMe_2)_5]Cl$[a]	1005	2.15
β-$[Os_2(S_2CNMe_2)_5]Cl$[b]	865	2.33
α-$[Ru_2(S_2CNMe_2)_5]BF_4$[c]	1040	2.40
β-$[Ru_2(S_2CNMe_2)_5]BF_4$[c]	950	2.18

[a] Determined in CH_2Cl_2; from ref 7. [b] Determined in CH_3CN; this work. [c] Determined in $CHCl_3$; from ref 8.

supplementary materials, respectively. A table of observed and calculated structure factors is available as supplementary material. Figure 2 presents an ORTEP perspective of the molecular structure of the cation and shows the labeling scheme.

Results and Discussion

In this paper we report three aspects of osmium dithiocarbamate chemistry. First, the stereochemistry of the bimetallic complex $[Os_2(S_2CNMe_2)_5]^+$ is discussed and results are presented that demonstrate the existence of two isomers; second, the single-crystal X-ray results are reported for a novel selenodithiocarbamate complex of osmium and are compared to those of the related trithiocarbamate complexes; and, third, the dynamic NMR properties of several tris(dithiocarbamate) complexes of osmium(III) are reported and related to the general class of stereochemically nonrigid tris(dithiocarbamate) complexes.

Stereochemistry of $[Os_2(S_2CNMe_2)_5]Cl$. The synthesis and characterization of this complex have been previously reported,[7] but its stereochemistry was not determined. It is likely that the Os complex exhibits either the α or β stereochemistry. These stereochemistries are both known for the analogous ruthenium complexes by X-ray structure determinations[8,24-26] and are shown in structures **3** and **4**. Hendrickson et al. reported that α-$[Ru_2(S_2CNMe_2)_5]^+$ thermally isomerizes into the β form with a first-order rate constant of 1×10^{-4} s^{-1} at 60 °C in $CHCl_3$ solution.[27,28] A ^1H NMR experiment was therefore carried out with $[Os_2(S_2CNMe_2)_5]^+$ in order to see if a similar isomerization occurred. The results of this experiment (CD_3CN solvent, 78 °C) are shown in Figure 1. The five signals observed in the initial spectrum decrease with time while five new signals appear. After ca. 118 h the isomerization is complete, and signals due to other isomers or decomposition products are completely absent. It is tempting to assign this process as the $\alpha \rightarrow \beta$ isomerization as observed with ruthenium; however, the stereochemistries cannot be assigned by ^1H NMR spectral analysis. The spectra of the α and β ruthenium complexes are simply too different from those of the osmium complexes to permit a correlation.

A comparison of the near-IR spectra of α- and β-$[Ru_2(S_2CNMe_2)_5]^+$ with those of the two osmium isomers reveals broad absorption bands in each case. For the ruthenium complexes, a shift to shorter wavelength is observed upon going from the α to the β isomer. This same trend is observed with osmium if one assumes that the thermal isomerization is $\alpha \rightarrow \beta$. These results are shown in Table III and support this assignment. The nature of the electronic transition responsible for these bands is uncertain; however, they are characteristic of the bimetallic complexes. No near-IR absorptions are observed for any of the monomeric dithiocarbamate complexes of Fe, Ru, or Os.

A kinetic analysis of the $\alpha \rightarrow \beta$ isomerization was carried out by plotting the disappearance of α-$[Os_2(S_2CNMe_2)_5]^+$ with time. Concentrations were measured by integration of the NMR signals. A plot of ln N_α, where N_α is the mole fraction of the α isomer, vs. time gives a linear relationship (Figure 4S in the supplementary material), indicating that the isomerization is first order. The first-order rate constant is 5×10^{-6} s^{-1} at 78 °C and may be compared with the value of 1×10^{-4} s^{-1} at 60 °C reported for ruthenium.[27,28] Since metal–sulfur bonds must be broken in order for the isomerization to occur, it is reasonable that the osmium complexes isomerize more slowly than their ruthenium analogues. The above observations show that the chemistry of the bimetallic $[Os_2(S_2CNR_2)_5]^+$ complexes is very similar to that of their ruthenium analogues.

Synthesis and Structure of $[Os_2(SeS_2CNMe_2)_2(S_2CNMe_2)_3]PF_6$. The reaction of $Os(S_2CNR_2)_3$ (R = Me or Et) with elemental sulfur in refluxing dimethylformamide yields two complexes that contain the trithiocarbamate ligand.[2] These complexes, $[Os_2(S_3CNR_2)_2(S_2CNR_2)_3]^+$ and $Os_2(S_3CNR_2)(S_5)(S_2CNR_2)_3$, have structures **1** and **2** as determined by single-crystal X-ray diffraction.[2] The existence of the trithiocarbamate ligand and an understanding of its reaction chemistry are important because this ligand has been proposed to be an important intermediate in the acceleration of rubber vulcanization.[4,5] For insight into the mechanism of sulfur incorporation, the reaction of $Os(S_2CNMe_2)_3$ with elemental selenium was studied. The only product isolated from this reaction in pure crystalline form was $[Os_2(SeS_2CNMe_2)_2(S_2CNMe_2)_3]PF_6$, **5**, although other unidentified products were obviously formed. The workup and purification procedures are quite involved, and only low yields of the selenium analogues of complexes **1**, **2**, and **5** have been obtained. A single-crystal X-ray analysis of **5** was carried out in order to determine the location of the selenium atoms and the overall stereochemistry of the complex.

The structure of **5** is very similar to that of **1** except that the two selenium atoms were located in the bridging positions. The molecular structure of **5** is shown in Figure 2.

The crystal structure of **5** consists of well-separated $[Os_2(SeS_2CNMe_2)_2(S_2CNMe_2)_3]^+$ cations and PF_6^- anions. The shortest interionic distance not involving an H atom is 3.11 (5) Å between C56A and F2. Selected distances and angles are presented in Table IV.

The Os–Os distance of 2.836 (1) Å in **5**, though slightly longer than that in **1** (2.792 (1) Å), is indicative of metal–metal bonding. The Os–S(SCNMe)$_2$ distances and the $S_2CNMe_2^-$ ligand geometries are nearly identical with those of **1** (Os–S average 2.421 (8) and 2.417 (3) Å; S–Os–S intraligand "bite" angle average 71.4 (2) and 72.0 (1)° in complexes **5** and **1**, respectively). The nonbridging Os–S(SeSCNMe$_2$) distances in **5** (average 2.373 (8) Å) are shorter than the Os–S(SCNMe$_2$) distances. The bridging Os–Se(S_2CNMe_2) distances in **5** (average 2.372 (4) Å) are longer than the corresponding bridging Os–S(S_2CNMe_2) distances in **1** (average 2.275 (3) Å), although the Os–X–Os angles are slightly smaller [average 73.4 (2) and 75.7 (1)° in **5** (X = Se) and **1** (X = S), respectively]. The S–C distances (average 1.71 (3) Å) and the S_2C–N distances (average 1.36 (4) Å) in **5** are similar to those found in **1**. The average Se–S distance of 2.26 (1) Å in the two $SeS_2CNMe_2^-$ ligands compares favorably with those in selenium xanthates and selenocarbamates, which range from 2.170 to 2.323 Å,[29] and with the average value of 2.25 Å found for a number of compounds containing Se–S bonds.[29-32] The average S–S distance in **1** is 2.154 (5) Å,

(24) Mattson, B. M.; Heiman, J. R.; Pignolet, L. H. *Inorg. Chem.* **1976**, *15*, 564.
(25) Given, K. W.; Mattson, B. M.; McGuiggan, M. F.; Miessler, G. L.; Pignolet, L. H. *J. Am. Chem. Soc.* **1977**, *99*, 4855.
(26) Raston, C. L.; White, A. H. *J. Chem. Soc., Dalton Trans.* **1975**, 2418.
(27) Hendrickson, A. R.; Hope, J. M.; Martin, R. L. *J. Chem. Soc., Dalton Trans.* **1976**, 2032.
(28) Hendrickson, A. R.; Martin, R. L.; Taylor, D. *Aust. J. Chem.* **1976**, *29*, 269.
(29) Brondmo, N. J.; Esperas, E.; Husebye, S. *Acta Chem. Scand., Ser. A* **1975**, *A29*, 93 and references cited therein.
(30) Hauge, S. *Acta Chem. Scand., Ser. A* **1979**, *A33*, 313.

Table IV. Selected Distances and Angles in $[Os_2(SeS_2CNMe_2)_2(S_2CNMe_2)_3]PF_6$

		Distances, Å			
Os1-Os2	2.836 (1)	Os2-S2	2.374 (8)	S4-C34	1.65 (4)
Os1-Se1	2.370 (4)	Os2-S4	2.371 (8)	S5-C56	1.71 (3)
Os1-Se2	2.373 (4)	Os2-S9	2.438 (8)	S6-C56	1.61 (3)
Os2-Se1	2.373 (4)	Os2-S10	2.428 (8)	S7-C78	1.71 (3)
Os2-Se2	2.370 (4)	Se1-S1	2.25 (1)	S8-C78	1.70 (3)
Os1-S5	2.414 (8)	Se2-S3	2.27 (1)	S9-C91	1.76 (5)
Os1-S6	2.396 (8)	S1-C12	1.69 (3)	S10-C91	1.77 (5)
Os1-S7	2.437 (8)	S2-C12	1.77 (3)	C12-N12	1.37 (4)
Os1-S8	2.415 (8)	S3-C34	1.69 (4)	C34-N34	1.43 (4)
C56-N56	1.49 (4)	C78-N78	1.33 (4)	C91-N91	1.16 (5)
		Angles, deg			
Se1-Os1-Se2	106.6 (2)	S9-Os2-S10	71.8 (3)	Se2-S3-C34	100 (1)
Se1-Os2-Se2	106.6 (2)	Os1-Se1-Os2	73.4 (1)	S1-C12-S2	124 (2)
S5-Os1-S6	71.1 (3)	Os1-Se2-Os2	73.4 (1)	S3-C34-S4	131 (2)
S7-Os1-S8	71.4 (3)	Os1-Se1-S1	111.8 (3)	S5-C56-S6	115 (2)
Se1-Os2-S2	91.3 (2)	Os2-Se1-S1	104.2 (3)	S7-C78-S8	112 (2)
Se2-Os2-S4	91.4 (3)	Se1-S1-C12	105 (1)	S9-C91-S10	108 (3)

much shorter than the Se–S distance in **5**. Indeed, all bonded distances involving Se in **5** are ca. 0.10 Å longer than the corresponding distances involving S in **1**. This is due to the difference in covalent radii between Se and S, which is 0.13 Å.[33] This supports the assignment of Se to the bridging positions in **5**.

The S_2CN grouping of the three $S_2CNMe_2^-$ ligands and the two $SeS_2CNMe_2^-$ ligands all form planar groupings within experimental error. Additionally, the core atoms of Os1, Os2, Se1, and Se2 form a planar grouping, as was found with the Os_2S_2 core atoms of **1** and **2**.

The location of Se only in the bridging positions of **5** suggests that the addition of Se or S to $Os(S_2CNR_2)_3$ occurs via a mechanism that involves initial bonding of S_8 or Se_8 or fragments thereof by Os. This result supports the mechanism previously proposed by us that involves the μ-S atoms coming from the μ-S_5 ligand in complexes such as **2**.[2]

Dynamic NMR of $Os(S_2CNR_2)_3$. The $Os(S_2CNR_2)_3$ complexes are low-spin d^5 both in the solid state and in solution, and their ^1H NMR spectra consist of isotropically shifted resonances.[11,34] The symmetrically substituted complex $Os(S_2CNBz_2)_3$ possesses D_3 symmetry, which requires the CH_2 protons to be in diastereotopic environments.[35] These protons can therefore serve as probes for metal-centered inversion.[15-17,36] At temperatures where optical inversion is slow on the ^1H NMR time scale, two well-separated resonances are observed. This is illustrated in the +3 °C spectrum of Figure 5S of the supplementary material, which shows the ^1H NMR traces for the N-CH_2 resonances of $Os(S_2CNBz_2)_3$ in acetone-d_6 at various temperatures. As the temperature is increased, the two resonances broaden and coalesce into a single line at ca. +46 °C. Similar behavior has also been observed for $Fe(S_2CNBz_2)_3$[15] and $Ru(S_2CNBz_2)_3$.[17]

As a test for the possibility that ligand dissociation could be responsible for the observed NMR behavior, $Os(S_2CNMe_2)_3$ and $Os(S_2CNEt_2)_3$ were mixed in CD_2Cl_2 solution. No signs of mixed-ligand complexes could be detected by ^1H NMR after 12 h at 30 °C. The observation that ligand exchange is therefore slow on the NMR time scale is consistent with the results reported for $Ru(S_2CNR_2)_3$[17] and indicates that inversion and its associated geometrical isomerization are intramolecular for $Os(S_2CNBz_2)_3$. A computer line-shape

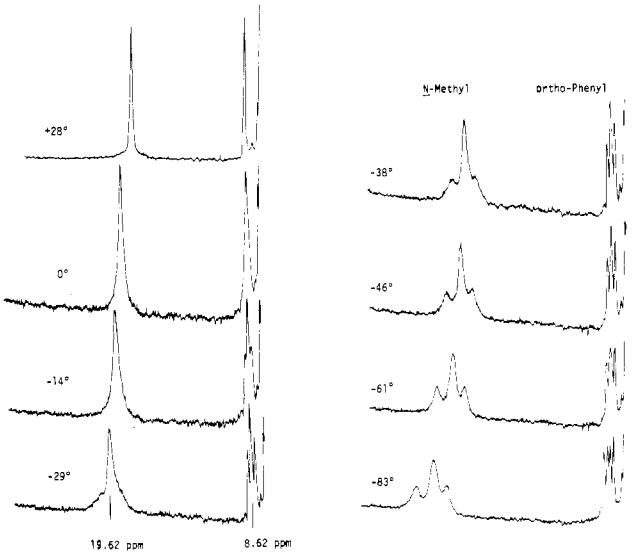

Figure 3. DNMR spectra of the N-CH_3 and ortho phenyl resonances of $Os(S_2CNMePh)_3$ recorded with CD_2Cl_2 as solvent.

calculation, Figure 5S, confirms that the coalescence results from a kinetic exchange process and that metal-centered inversion is indeed rapid on the NMR time scale at temperatures above ca. 50 °C.

The unsymmetrically substituted complex $Os(S_2CNMePh)_3$ has the additional features of cis and trans geometrical isomers. Although its ^1H NMR spectrum is more complex, its temperature dependence is consistent with that obtained for $Os(S_2CNBz_2)_3$. At temperatures below ca. −80 °C, four distinct resonances (one for the cis isomer and three for the trans isomer) for the ortho protons of the phenyl ring occur at ca. 9.00 ppm (−83 °C spectrum of Figure 3). The assignment of these resonances to the ortho protons of the phenyl ring was made by careful integration of the aromatic region. Although four N-CH_3 resonances are also expected at temperatures below ca. −80 °C, only three resonances with area 1:2:1 could be resolved at ca. 24.17 ppm. Two peaks are accidentally degenerate. The DNMR spectra of these resonances are shown in Figure 3. As the temperature is raised, the middle two ortho-proton resonances coalesce (ca. −60 °C) as well as the outer two N-CH_3 peaks (ca. −30 °C). This type of behavior has been observed for other unsymmetrically substituted $M(S_2CNRR')_3$ complexes[12-17] and is ascribed to a process whereby two of the trans-N-CH_3 (or ortho-proton) environments are interchanged, leaving the cis and other trans environments unchanged. Geometric isomerization (such as would result from rapid S_2C–N bond rotation) cannot cause

(31) Erickson, R. *Acta Chem. Scand., Ser. A* **1975**, *A29*, 517.
(32) Maroy, K. *Acta Chem. Scand.* **1972**, *26*, 36.
(33) Pauling, L. "The Nature of the Chemical Bond", 3rd ed.; Cornell University Press: Ithaca, NY, 1960; p 225.
(34) Holm, R. H. *Acc. Chem. Res.* **1969**, *2*, 307.
(35) Mislow, K.; Rabin, M. *Top. Stereochem.* **1965**, *1*, 1.
(36) Optical inversion in tris chelate complexes is the interconversion of Δ and Λ isomers. This process has been described in ref 18.

Table V. Kinetic Parameters for Intramolecular Metal-Centered Inversion for Tris(dithiocarbamato) Complexes of Iron, Ruthenium, and Osmium

complex[a]	$\Delta H^{\ddagger}$, kcal/mol	$\Delta S^{\ddagger}$, eu	$\Delta G^{\ddagger}$, kcal/mol[b] (T, °C)
$Fe(S_2CNBz_2)_3$[c]	10.3 ± 1.0	4.1 ± 5.0	9.3 ± 0.2 (−54)
$Fe(S_2CNMePh)_3$[c]	8.7 ± 1.0	1.7 ± 5.0	8.9 ± 0.2 (−80)
$Fe(S_2CNMeBz)_3$[c]	9.5 ± 1.5	3[g]	8.5 ± 0.2 (−86)
$Ru(S_2CNBz_2)_3$[d]	11.6 ± 1	−7 ± 5	13.8 ± 0.2 (+42)
$Ru(S_2CNMePh)_3$[d]	10.1[f]	−7.5[g]	12.1 ± 0.2 (+9)
$Ru(S_2CNMeBz)_3$[d]	11.1[f]	−7.5[g]	13.3 ± 0.2 (+15)
$Os(S_2CNBz_2)_3$[e]	11.8 ± 1.5	−9 ± 6	14.6 ± 0.2 (+46)
$Os(S_2CNMePh)_3$[c]			10.9 ± 0.5[h]

[a] Fe complexes from ref 15; Ru complexes from ref 17. [b] Given at a temperature where k is measured directly by line-shape analysis. [c] CD_2Cl_2 solution. [d] $CDCl_3$ solution. [e] Acetone-d_6 solution. [f] No error limits given. [g] Assumed values of $\Delta S^{\ddagger}$ used in the calculation of $\Delta H^{\ddagger}$. [h] Estimated value determined from coalescence of ortho protons at −61 °C and N-CH_3 peaks at −29 °C (see Results and Discussion).

this result since simultaneous collapse of all four ortho-proton (or N-CH_3) resonances would have to occur. Values of 11.1 and 10.6 kcal/mol were estimated for $\Delta G^{\ddagger}$ at the coalescence temperatures of the N-CH_3 and ortho-proton resonances, respectively, and the similarity of these values (assuming $\Delta S^{\ddagger}$ is small) indicates that the same process is responsible for the coalescence of these two sets of resonances. These values are also reasonably close to the activation parameters of $Os(S_2CNBz_2)_3$ ($\Delta H^{\ddagger}$ = 11.8 kcal/mol, $\Delta G^{\ddagger}$ (−45 °C) = 13.9 kcal/mol, and this evidence supports the conclusion that the process which is responsible for the coalescences observed in $Os(S_2CNMePh)_3$ is the same one which causes coalescence of the N-CH_2 resonances in $Os(S_2CNBz_2)_3$. The coalescence observed for $Os(S_2CNBz_2)_3$ shows that metal-centered inversion must accompany this process. Because of these observations and the similarity of these results to those obtained for $Ru(S_2CNMeBz)_3$[14] and $Ru(S_2CNBz_2)_3$,[17] for which the mechanism of rearrangement has been clearly demonstrated, one can conclude that the osmium complexes rearrange by the trigonal twist mechanism. The detailed arguments that lead to this conclusion have been thoroughly discussed elsewhere.[18] At temperatures above −14 °C, S_2C–N bond rotation becomes fast on the ^1H NMR time scale and causes coalescence of all remaining N-CH_3 and ortho-proton resonances.

Kinetic parameters for metal-centered inversion were determined by a total line-shape analysis of the ^1H NMR spectra of $Os(S_2CNBz_2)_3$ recorded at several temperatures (see Experimental Section). These results are shown in Table V along with parameters for similar iron and ruthenium complexes. The entropy of activation, $\Delta S^{\ddagger}$, is consistent with values obtained for other complexes known to rearrange by the trigonal twist mechanism.[15,16,18,37-39] These values are usually near zero or slightly negative. The values of $\Delta H^{\ddagger}$ and $\Delta G^{\ddagger}$ compare favorably with those obtained for a number of $Ru(S_2CNR_2)_3$ complexes that rearrange by the trigonal twist mechanism. A relationship has been found to exist between the difference in ligand field stabilization energy (LFSE) for trigonal-antiprismatic, TAP, and trigonal-prismatic, TP, geometries and the activation energy for metal-centered inversion.[18] Higher activation energies were found to correspond to larger values of ΔLFSE = LFSE(TAP) − LFSE(TP). This relationship is exemplified well by the $M(S_2CNR_2)_3$ complexes, where M = Fe, Ru, and Os. The values of $\Delta H^{\ddagger}$ for a series of ruthenium and osmium tris(dithiocarbamate) complexes are generally higher than those for the corresponding iron complexes. This result is as expected due to the larger values of Dq and ΔLFSE associated with second- and third-row metal complexes.

The observation that the osmium complexes rearrange at rates that are comparable to those of their ruthenium analogues is somewhat unexpected since it is generally assumed that tris chelates of the heavier transition metals within a group are more inert to rearrangement.[18,37] Also, this observation is consistent with the proposal that the $\alpha \rightarrow \beta$ rearrangement of $[M_2(S_2CNR_2)_5]^+$ complexes occurs by M–S bond rupture (vide supra). If a non-bond-breaking mechanism was operative in the $\alpha \rightarrow \beta$ isomerization, the rates for Ru and Os should be comparable on the basis of the results in Table V. However, the observed rates differ by nearly 3 orders of magnitude with that of Ru being faster than that of Os. This is consistent with a M–S bond-rupture mechanism because Os–S bonds are stronger than Ru–S bonds.

Acknowledgment. This research was supported by the National Science Foundation. We also thank Engelhard Industries for a generous loan of OsO_4 and the St. Olaf College Computer Center for assistance with the computer programs used for line-shape analyses.

Registry No. **3**, 83928-04-5; **4**, 69493-68-1; **5**, 83928-06-7; $Os(S_2CNBz_2)_3$, 83928-02-3; $Os(S_2CNMePh)_3$, 83928-03-4; $Fe(S_2CNBz_2)_3$, 23451-11-8; $Fe(S_2CNMePh)_3$, 15635-69-5; $Fe(S_2CNMeBz)_3$, 23674-41-1; $Ru(S_2CNBz_2)_3$, 51751-58-7; $Ru(S_2CNMePh)_3$, 51751-60-1; $Ru(S_2CNMeBz)_3$, 51751-59-8.

Supplementary Material Available: Figures 1S–5S, showing ln $H_{1/2}$ vs. $1/T$, $\Delta\nu$ vs. $1/T$, an Eyring plot, ln N_α vs. time, and ^1H NMR traces as a function of temperature for $Os(S_2CNBz_2)_3$, and Tables IS and IIS, showing structure factor amplitudes and anisotropic thermal parameters for $[Os_2(SeS_2CNMe_2)_2(S_2CNMe_2)_3]PF_6$ (21 pages). Ordering information is given on any current masthead page.

(37) Eaton, S. S.; Eaton, G. R.; Holm, R. H.; Muetterties, E. L. *J. Am. Chem. Soc.* **1973**, *95*, 1116 and references cited therein.
(38) Serpone, N.; Bickley, D. G. *Prog. Inorg. Chem.* **1972**, *17*, 391.
(39) Eaton, S. S.; Hutchinson, J. R.; Holm, R. H.; Muetterties, E. L. *J. Am. Chem. Soc.* **1972**, *94*, 6411.